ARTICLE

Immunotherapy during the acute SHIV infection of macaques confers long-term suppression of viremia

Yoshiaki Nishimura[1], Olivia K. Donau[1], Joana Dias[2], Sara Ferrando-Martinez[2], Eric Jesteadt[1], Reza Sadjadpour[1], Rajeev Gautam[1], Alicia Buckler-White[1], Romas Geleziunas[3], Richard A. Koup[2], Michel C. Nussenzweig[4,5], and Malcolm A. Martin[1]

We report that combination bNAb immunotherapy initiated on day 3 post-infection (PI) maintained durable CD8^{+} T cell–mediated suppression of SHIV$_{AD8}$ viremia and preinoculation levels of CD4^{+} T cells in 9 of 13 treated monkeys during nearly 6 yr of observation, as assessed by successive CD8^{+} T cell–depletion experiments. In an extension of that study, two treatment interventions (bNAbs alone or cART plus bNAbs) beginning on week 2 PI were conducted and conferred controller status to 7 of 12 monkeys that was also dependent on control mediated by CD8^{+} cells. However, the median time to suppression of plasma viremia following intervention on week 2 was markedly delayed (85 wk) compared with combination bNAb immunotherapy initiated on day 3 (39 wk). In both cases, the principal correlate of virus control was the induction of CD8^{+} T cellular immunity.

Introduction

In most untreated individuals, HIV-1 infection leads to high levels of sustained virus replication, unremitting and irreversible depletion of CD4^{+} T cells, and ultimately symptomatic immunodeficiency with associated opportunistic infections, leading to a fatal clinical outcome. A small number of HIV-1 infected persons (elite controllers) are able to suppress viremia for prolonged periods of time, a phenomenon that is associated with the activity of virus-specific CD8^{+} T cells (Betts et al., 2006; Deeks and Walker, 2007; Pereyra et al., 2008).

Potent broadly neutralizing antibodies (bNAbs) have been used to prevent and treat lentivirus infections in macaques and humans (Borducchi et al., 2018; Caskey et al., 2015, 2017; Gautam et al., 2016, 2018; Hessell et al., 2016; Ledgerwood et al., 2015; Lu et al., 2016; Lynch et al., 2015; Moldt et al., 2012; Nishimura et al., 2017; Shingai et al., 2013). We previously reported that the administration of combination bNAbs alone during early simian immunodeficiency virus (SIV)/HIV chimeric virus (SHIV) infections of rhesus macaques can induce durable control of virus replication (Nishimura et al., 2017). In that study, 13 macaques were inoculated by the intrarectal (i.r.) or i.v. route with SHIV$_{AD8-EO}$, and beginning on day 3 after virus challenge, they received a single course of three weekly i.v. infusions (on days 3, 10, and 17) of combination 10–1074 (Mouquet et al., 2012) plus 3BNC117 (Scheid et al., 2011) bNAbs. All of the treated monkeys

controlled virus replication for varying periods of time (8–26 wk), and when bNAb levels waned, rebound viremia occurred in 12 of the 13 animals, reaching peak levels of 10^5 RNA copies/ml in several macaques. During an initial 100–140-wk observation period, six of these animals (three challenged i.r. and three challenged i.v.), designated "controllers," suppressed plasma viremia to undetectable levels and durably maintained circulating CD4^{+} T cell numbers (Fig. 1). A CD8^{+} T cell–depleting mAb, specific for the CD8α chain, was administered to all six controller animals between weeks 48 and 131 after virus challenge (Fig. 1, A–F; left red arrows), resulting in transient bursts of plasma viremia that were rapidly resolved in five of the six monkeys. Quantitative virus outgrowth assays, performed before CD8^{+} T cell depletion, indicated that <1 cell/10^6 circulating CD4^{+} T cells was releasing infectious virions in these macaques. In the final reported experiment, anti-CD8β, which depletes CD8^{+} T cells but not natural killer, natural killer T, or γδ T cells, was administered to three controller animals between weeks 136 and 150 after SHIV$_{AD8-EO}$ challenge. Although not as potent in vivo as the anti-CD8α mAb, the anti-CD8β mAb infusion induced an immediate increase in plasma viremia (Fig. 1, A, D, and F; blue arrows). In that study, control macaques treated for 15 wk with a combination antiretroviral therapy (cART) regimen also initiated on day 3 after SHIV challenge, exhibited sustained
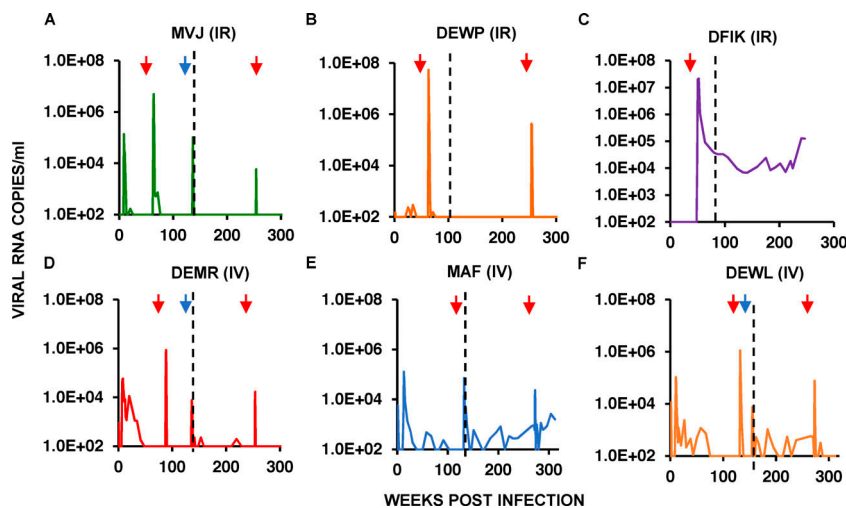
Figure 1. **Establishment of controller status following a 2-wk course of combination bNAb therapy beginning on PI day 3 in rhesus macaques inoculated with SHIV$_{AD8-EO}$. (A–F)** Plasma virus loads in six controller bNAb recipients over a 250–315-wk observation period are shown. Red arrows in each panel indicate the time of the anti-CD8α–depleting mAb MT807R1 infusion. Blue arrows for macaques MVJ, DEMR, and DEWL denote infusion of the anti-CD8β–depleting mAb CD8b255R1. The vertical dotted lines separate the previously reported results (Nishimura et al., 2017) from new data collected during the past 2.5–3.5 yr. IR, intrarectally; IV, intravenously.

plasma viremia upon treatment interruption, and none became virus controllers (Nishimura et al., 2017). These results indicated that passive combination bNAb immunotherapy, initiated during early acute infection, induces potent CD8$^+$ T cell immunity able to durably suppress virus replication.

Here, we have extended these initial findings by (1) monitoring the virologic and CD4$^+$ T cell status of the original "day 3" treated controller monkeys during an additional 2.5–3.5-yr period and (2) initiating a new immunotherapy regimen in which the effects of combination bNAb alone or cART plus bNAb treatment began at the more clinically relevant week 2 after the SHIV infection time point.

Results

Combination bNAb immunotherapy initiated on day 3 postinfection (PI) suppressed SHIV$_{AD8}$ replication in 9 of 13 macaques for 6 yr and was mediated by CD8$^+$ T cells

As shown in Fig. 1, A, B, and D–F, five of the original six controller animals continued to control plasma viremia between weeks 110 and 315 PI. 6 yr after the initiation of bNAb treatment in the day 3 infection cohort, five of the original six controller monkeys also maintained physiological levels of circulating CD4$^+$ T cells (Fig. S1, A–E). As shown in Fig. 1 C, the sixth controller animal (DFIK), which did not exhibit virus rebound following the waning of the initial 3-wk bNAb treatment, was also unable to recontrol virus replication following the administration of the depleting anti-CD8α mAb at week 48 PI. The remaining five day 3 controllers received a final anti-CD8α mAb infusion at PI week 250 or 270, and all experienced another transient burst of viremia that was rapidly suppressed to background levels in four of the five animals (Fig. 1, A, B, and D–F; red arrows on right).

Seven of the original recipients of combination bNAb immunotherapy on PI day 3 had not durably suppressed plasma viremia by week 110 or 140 PI, when the original report was published, and were designated progressors. Interestingly, during the fourth and fifth years after bNAb immunotherapy initiation, three of these seven original progressors (DFFX, DFKX, and DEHW) suppressed virus replication and became late controllers (Fig. 2, A–C). As observed with the original six

controller animals, infusion of depleting anti-CD8α mAb into the three late controllers at week 285 or 315 after the virus challenge also resulted in a transient burst of viremia. Three of the other four progressors developed clinical immunodeficiency and were euthanized between years 2 and 5 PI (Fig. 2, D–G). Thus, 9 of the original 13 animals administered combination bNAbs starting on day 3 PI, were able to control viremia in a CD8$^+$ T cell–dependent manner after early antibody therapy.

Phylogenetic analysis of SHIV *env* gene sequences from the six early controllers collected during peak viremia after the first anti-CD8α antibody treatment (weeks 70–130 PI), from the three late controllers, and from the four progressors (both between weeks 110 and 150 PI) is shown in Fig. S2. Consistent with persistent viremia and viral replication, the *env* sequences from the four progressor monkeys exhibited the greatest diversity, while the six early controller animals were least diverse. The diversity of *env* genes from the late controllers was intermediate, an indicator of sustained, but weaker, CD8$^+$ T cell–mediated pressure to suppress the ongoing viral infection.

Initiation of bNAb only or cART plus bNAb treatment regimens on week 2 PI resulted in controller status in 7 of 12 monkeys

To assess whether bNAb intervention at day 3 PI, which ultimately resulted in sustained control of virus replication in 9 of 13 macaques, would be effective when initiated at a more clinically relevant time, two groups of SHIV-infected monkeys were treated with bNAbs alone or with cART plus bNAbs starting at week 2 PI. The first cohort of six infected animals received three infusions at biweekly intervals of combination 10–1074 plus 3BNC117 bNAbs (10 mg/kg each) starting 14 d after infection, at the time of peak viremia (10^7–10^8 RNA copies/ml; Fig. 3 A). This bNAb regimen modestly suppressed the initial virus replication in five of the six animals by week 10 PI. In one monkey (DG34; Fig. 3 D), bNAb administration reduced plasma viremia below the level of detection, whereas immunotherapy was less effective in the other recipients. Following a virus rebound lasting 15 wk, macaque DG34 controlled SHIV replication to undetectable levels by week 30 PI (Fig. 3 D). Three other recipients of combination bNAb treatment beginning at week 2 also controlled virus replication, but only after 90–150 wk after infection (Fig. 3, B, C,
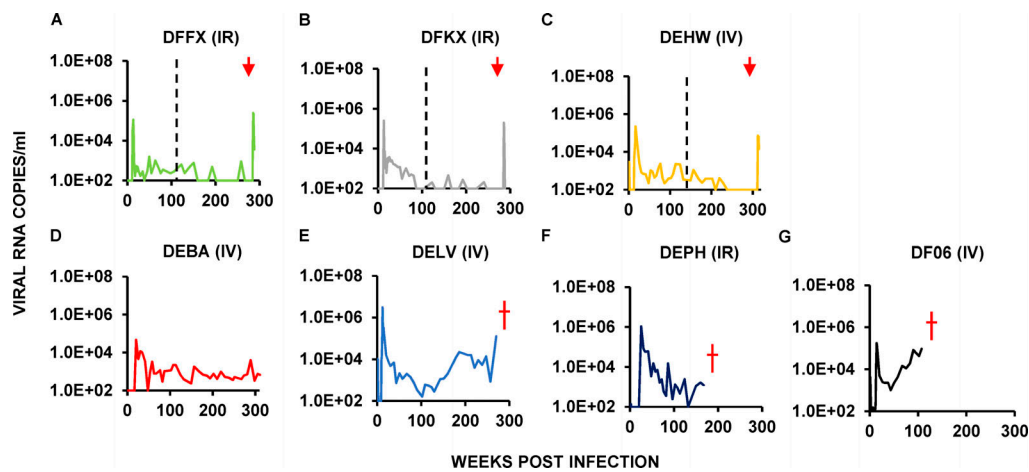
Nishimura et al.
NAb treatment generates durable cellular immunity

Journal of Experimental Medicine   2 of 8
https://doi.org/10.1084/jem.20201214

Figure 2. Virus replication in three late controller and four progressor macaques inoculated with SHIV$_{AD8-EO}$ and administered a 2-wk course of combination bNAb therapy beginning on day 3 PI. (A–G) Plasma virus loads in three late controller macaques (A–C) and four progressor macaques (D–G) are shown over a 140–350-wk period. Red arrows indicate the time of the anti-CD8α–depleting mAb MT807R1 infusions. The three progressors that developed AIDS and were euthanized are indicated (red †). The vertical dotted lines separate the previously reported results (Nishimura et al., 2017) from new data collected during the past 2.5–3.5 yr. IR, intrarectally; IV, intravenously.

and E). Infusion of anti-CD8α mAb into these four controller monkeys at week 162 PI elicited transient bursts of plasma viremia, peaking at 10^6–10^7 RNA copies/ml (Fig. 3, B–E). Circulating CD4+ T cell levels in all four controllers were stable during the 3-yr observation period, although transient declines attending the CD8 depletions were observed in these monkeys (Fig. S1, F–I). The two progressor macaques in this treatment group continued to generate progeny virions at set point levels of 10^3–10^4 RNA copies/ml during the post-therapy period (Fig. 3, F and G), and one (DFA3) exhibited a slow continuous reduction of CD4+ T cells that was associated with a rising viral set point (Fig. S1 J).

The second group of six animals received daily cART therapy for 8 wk beginning at week 2 PI and a biweekly, three-infusion course of combination 10–1074 plus 3BNC117 bNAbs (10 mg/kg each) starting at week 9 PI; cART was discontinued at week 10 PI (Fig. 4 A). Peak levels of viremia ranged from 10^7 to 10^8 RNA copies/ml at the time of cART intervention and were rapidly suppressed to background levels between weeks 5 and 8 PI in all animals. The addition of combination bNAbs at week 9 extended the control of SHIV$_{AD8-EO}$ replication until weeks 17–26 PI, after which viral rebound occurred to the 10^4–10^5 viral RNA copies/ml range when antibody levels had declined below effective levels. Viremia was durably suppressed between weeks 70 and 160 PI in three of these macaques, which were designated controllers (Fig. 4, B–D). Administration of the depleting anti-CD8α mAb at week 200 to these three controller monkeys led to transient bursts of virus replication. As was observed with controllers induced by combination bNAb immunotherapy alone (Fig. S1, F–I), modest CD4 declines also accompanied the infusion of the anti-CD8 depleting antibody in the controller animals (Fig. S1, L–N).

The patterns of durable control were different when bNAb immunotherapy was initiated on day 3 or week 2 PI

Although bNAb treatment initiated on either day 3 or day 14 resulted in sustained suppression of SHIV$_{AD8-EO}$ infection in a

similar fraction of macaques, there were important differences between the two cohorts. Although the level of viremia on day 3 PI was, at most, 10^3–10^4 RNA copies/ml when combination bNAb immunotherapy was started, the viral loads on week 2 were 10^7–10^8 RNA copies/ml. This difference was reflected in (1) a relatively rapid and nearly complete resolution of rebound viremia for controller monkeys receiving bNAbs beginning on day 3 PI (Fig. 1, A–F) versus (2) a very long and drawn-out process, requiring, in some cases, 2 or 3 yr to achieve control status for both cohorts that received bNAbs starting at week 2 (Fig. 3, B, C, and E; and Fig. 4, B–D). As shown in Fig. 5, this difference is reflected in the median times for bNAb-induced controller status: 38.7 versus 86.9 and 82.5 wk for interventions at day 3 (bNAbs only), week 2 (bNAbs only), or week 2 (cART plus bNAbs), respectively. The three additional day 3 late controller monkeys achieved controller status at a median time of 159 wk after infection.

Assessment of CD8+ T cells in the LNs of SHIV$_{AD8}$ controller and progressor monkeys

As previously reported, controller or progressor monkeys that started bNAb immunotherapy on day 3 PI generated low levels of gp120 antibodies and minimal or no differences in anti-SIVmac239 Gag protein–mediated peripheral CD8+ T cell responses (Nishimura et al., 2017). To examine CD8+ T cell responses in lymphoid tissues in these treated macaques, we collected available superficial LNs from three controllers, two progressors, and four cART control animals on week 180 PI. As shown in Fig. S3 A, accumulation of follicular (f) CXCR5+ CD8+ T cells (Ferrando-Martinez et al., 2018; Petrovas et al., 2017) was observed in LNs in controller animals. Antiviral-specific CD8+ T cell responses were assessed by cytokine production and degranulation following stimulation with pooled SIVmac239 Gag peptides. The antiviral responses in both bulk and follicular CXCR5+ CD8+ T cells, residing in LNs from the four controller macaques, were higher than those collected from progressor or cART control monkeys
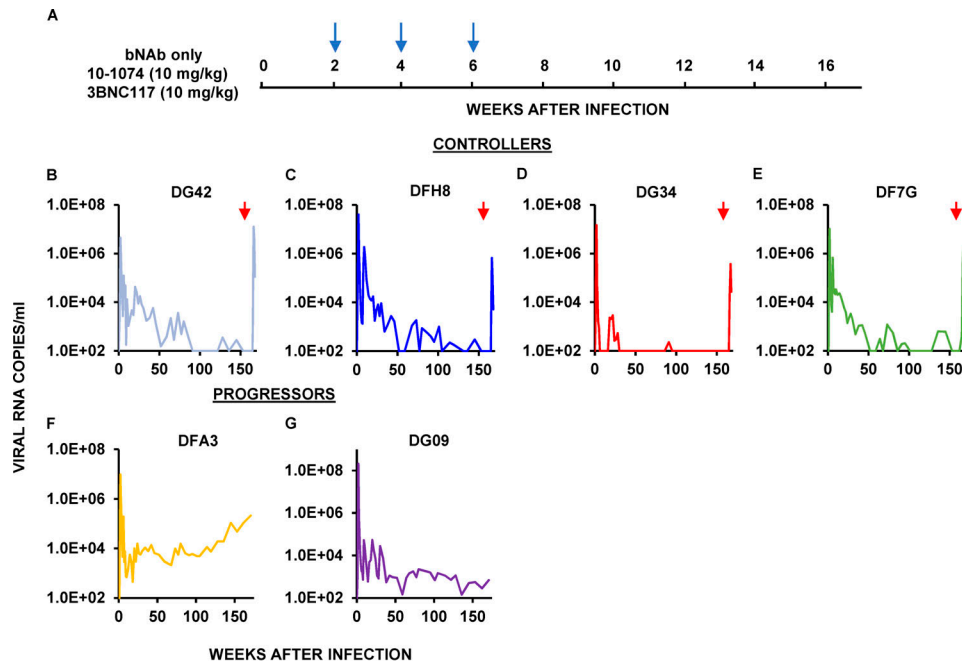
Figure 3. Establishment of controller status by a single biweekly three-infusion course of combination bNAb therapy beginning at week 2 PI in rhesus macaques inoculated with SHIV$_{AD8-EO}$. (A) Six rhesus macaques were inoculated i.r. with 1,000 TCID$_{50}$ of SHIV$_{AD8-EO}$ and treated with 10–1074 plus 3BNC117 (10 mg/kg of each) bNAbs at weeks 2, 4, and 6 PI (blue arrows), and their viral loads were monitored over a 170-wk period. **(B–G)** Plasma virus loads in four controller macaques (B–E) and two progressors (F and G) are shown. The red arrows indicate the times of anti-CD8α–depleting mAb MT807R1 infusion.

(Fig. S3 B). However, this was not statistically different because too few animals were analyzed (e.g., n = 2 for the progressor macaques). Polyfunctional analysis revealed that the controller animals had higher levels of virus-specific CD69⁺MIP-1β⁺CD107a⁺

and CD107a⁺ single-positive CD8⁺ T cells than progressors or cART control monkeys (Fig. S4). In contrast to animals administered bNAbs on day 3 PI, follicular CXCR5⁺ CD8⁺ T cells did not accumulate in the LNs of the controllers emerging following
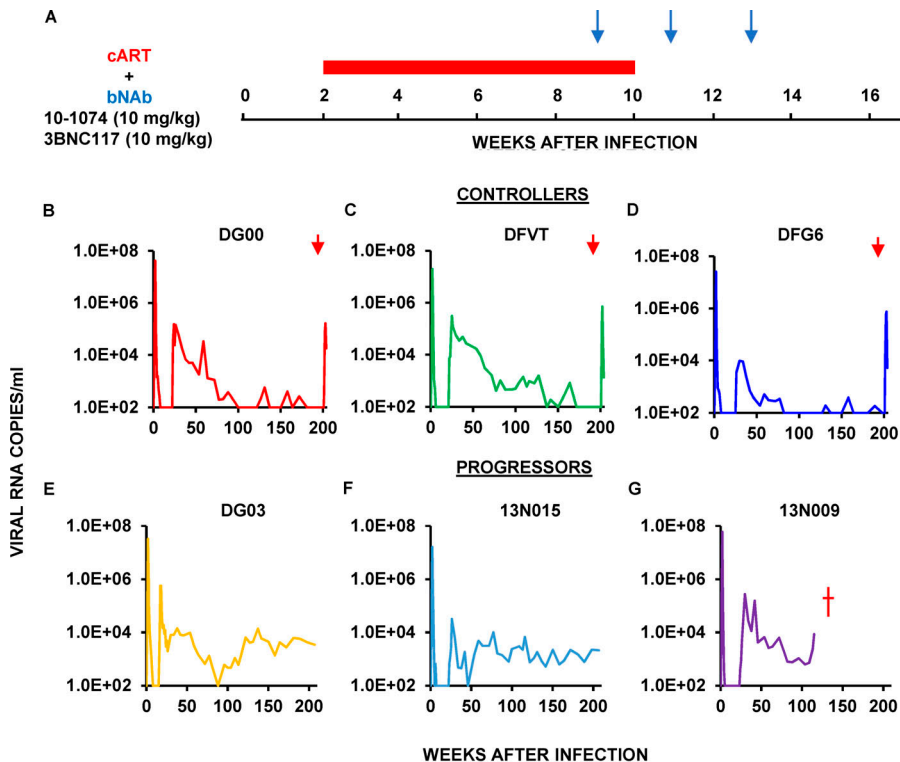

Figure 4. Establishment of controller status by successive cART therapy for 8 wk beginning at week 2 PI and combination bNAb treatment commencing on week 9 PI in rhesus macaques inoculated with SHIV$_{AD8-EO}$. (A) Six rhesus macaques were inoculated i.r. with 1,000 TCID$_{50}$ of SHIV$_{AD8-EO}$ and initially received daily cART therapy for 8 wk beginning at week 2 PI (red bar) and were then administered combination 10–1074 plus 3BNC117 bNAbs (10 mg/kg each) at weeks 9, 11, and 13 PI (blue arrows). **(B–G)** Plasma virus loads in three controller (B–D) and three progressor (E–G) macaques are shown. Red arrows indicate the times of the anti-CD8α–depleting mAb MT807R1 infusion.
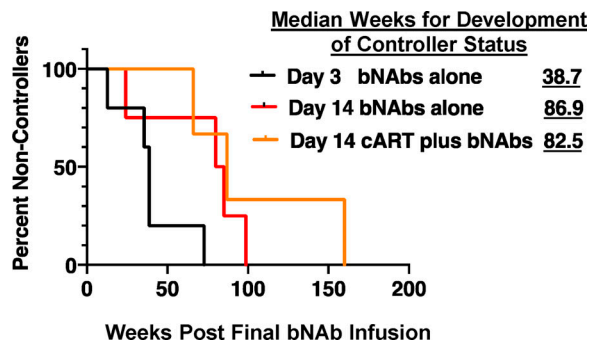
Figure 5. Achievement of controller status is delayed when antiretroviral treatment is initiated at week 2 PI. Kaplan–Meier analysis was used to assess the percentages of remaining non-controller monkeys following intervention with bNAbs at day 3 (*n* = 5 per group), cART plus bNAbs controllers at week 2 PI (*n* = 3), and bNAbs-only controllers also at week 2 PI (*n* = 4). The median numbers of weeks needed for the development of controller status are shown.

immunotherapy beginning on week 2 PI (Fig. S3 C). Gag-specific CD8+ T cell responses were indistinguishable in the LNs of seven controller and five progressor animals harvested between weeks 120 and 160 from the week 2 cohort (Fig. S3 D). The different CD8+ T cell profiles in LNs from controller monkeys emerging following bNAb immunotherapy initiated on day 3 and week 2 could reflect the higher initial viral loads and prolonged rebounds in the second cohort of monkeys, rendering them less responsive to the effects of bNAb therapy.

Discussion

Although we were unable to identify a distinctive T cell protective signature or mechanism conferring controller status on SHIV-infected rhesus macaques treated with combination anti–HIV-1 bNAbs starting on day 3 or week 2 PI, the consistent correlate of sustained virus suppression was the generation of CD8+ T cells, which persisted for 3–6 yr. In our earlier study, we reported that daily treatment of macaques with cART for only 15 wk, starting on day 3 PI, completely suppressed virus replication (Nishimura et al., 2017). However, all of these monkeys developed high levels of plasma viremia following the cessation of cART and none became controllers, indicating the critical role of bNAbs in conferring sustained repression of viremia.

Based on the data collected from 16 treated animals that became controller monkeys, we speculate that the establishment of long-term controller status in SHIV-infected monkeys may be facilitated and may be dependent on several critical factors. First, upon administration, bNAbs must potently suppress plasma viremia, preferably to undetectable levels, as was the case following their infusion on day 3 PI. When bNAb immunotherapy was initiated at week 2 PI, this degree of control was only observed in a single monkey (DG34; Fig. 3 D), which rapidly and potently suppressed virus replication that was sustained for an additional 2 yr. Second, although bNAb immunotherapy blocks neither virus replication nor progeny virion release from infected lymphoid cells, we previously proposed that bNAb administration in the presence of low levels of antigen production

could drive immune complex formation and lead to dendritic cell activation to produce a vaccinal effect. Third, the continuing production of viral antigens, further augmented by the rebounding viremia attending the decline of bNAbs to subtherapeutic levels, could additionally simulate antigen cross-presentation from dendritic cells, stimulating potent and sustained CD4+ and CD8+ T cell responses.

As noted from the results presented, the different patterns in establishing controller status following initiation of combination bNAb immunotherapy on day 3 and week 2 PI most likely reflect the high levels of circulating and cell-associated virus production at week 2 PI superimposed on a background of more extensive and possibly irreversible injury to the immune system. It should also be noted that identical bNAb dosing regimens (10 mg/kg) were administered to both groups of macaques, rather than infusing larger amounts (e.g., 30 mg/kg) of mAb at week 2 PI. The relatively low bNAb dose given to the monkeys at week 2 PI may have simply been inadequate to effectively control viral loads peaking in the range of 10^7–10^8 viral RNA copies/ml, leading to greater CD4+ T cell killing and the delayed development of a potent CD8+ T cell response. On the other hand, simply controlling viral loads to undetectable levels beginning at week 2 PI was insufficient in achieving controller status since the animals treated with cART between weeks 2 and 10 and then combination bNAbs starting at week 9 potently controlled the initial viremia to this degree but also experienced a nearly 2-yr delay in achieving controller status (Fig. 4). It is worth noting that a latent virus reservoir had been established in several of the day 3 controller monkeys despite the very early initiation of immunotherapy (Nishimura et al., 2017). It is therefore quite likely that such a reservoir was not only present but also had significantly increased in size by week 2 PI, further impeding systemic suppression of virus replication when bNAb treatment was started. That said, the burst of viremia following CD8 depletion at week 200 in all seven controller animals treated with bNAbs ± cART beginning at week 2 PI (Fig. 3 and Fig. 4) clearly indicates that potent systemic CD8+ T cell control of virus replication, nearly 4 yr after SHIV challenge, had been achieved.

It is still too early to tell whether bNAb treatment during the early phase of HIV-1 infections will also mediate sustained virus control in humans. Important differences between both SHIV and HIV-1 pathophysiology (e.g., the median time to immunodeficiency; 2 yr [nonhuman primate] versus 10 yr [human], respectively) as well as variable host responses to immunotherapy make such predictions difficult. Furthermore, direct mechanisms responsible for the development of potent antiviral CD8+ T cell responses remain to be elucidated. Nonetheless, consistent with the requirement for bNAb-induced CD8+ T cells for control of the robust SHIV$_{AD8}$ infection of macaques, chronically HIV-1–infected human recipients of combination bNAb therapy also exhibited increased CD8+ T cell responses (Niessl et al., 2020). In that study, CD8+ T cell responses peaked at 6–7 wk following the initiation of immunotherapy when bNAb levels in the blood were at their highest levels. Although we were unable to identify a distinctive protective mechanism responsible for subsequent sustained control of virus replication following the administration of combination anti–HIV-1 bNAbs

during the acute SHIV infection of rhesus macaques, the induction of CD8+ T cells was required in controllers from all cohorts.

Materials and methods
Animal experiments
25 male and female rhesus macaques (*Macaca mulatta*, 13 from previous study; Nishimura et al., 2017) of Indian genetic origin, ranging from 2 to 4 yr of age at the time of challenge, were maintained in accordance with the guidelines of the Committee on Care and Use of Laboratory Animals and were housed in a biosafety level 2 facility. All animal procedures and experiments were performed according to protocols approved by the Institutional Animal Care and Use Committee of the National Institute of Allergy and Infectious Diseases, National Institutes of Health. Phlebotomies, virus inoculations, mAb and cART infusions, and sample collections were performed as previously described (Endo et al., 2000; Nishimura et al., 2017; Shingai et al., 2012). All animals were negative for the major histocompatibility complex class I *Mamu-A*01*, *Mamu-B*08*, and *Mamu-B*17* alleles. Animals were not randomized, and the data collected were not blinded.

Virus challenge
The origin and preparation of the tissue culture–derived SHIV$_{AD8-EO}$ stock have been previously described (Shingai et al., 2012). 13 animals from the previous study (Nishimura et al., 2017) were challenged with SHIV$_{AD8-EO}$ i.v. (100 or 1,000 median tissue culture infectious dosage [TCID$_{50}$]) or i.r. (1,000 TCID$_{50}$) as previously described (Shingai et al., 2014). 12 new animals were challenged with 1,000 TCID$_{50}$ of SHIV$_{AD8-EO}$ i.r.

cART regimen
Six animals were treated with a three-drug (combination) ART regimen comprising two nucleoside RT inhibitors (tenofovir and emtricitabine) and one integrase inhibitor (raltegravir), starting at week 2 for 8 wk. The preformulated cocktail of tenofovir and emtricitabine was administered intramuscularly once a day at dosages of 20 mg/kg and 40 mg/kg. Raltegravir was administered orally (mixed with food) at a dosage of 200 mg twice a day.

Antibody administration
A combination of 3BNC117 (Scheid et al., 2011) and 10–1074 (Mouquet et al., 2012) anti–HIV-1 bNAbs (10 mg/kg each) was administered i.v. to individual animals biweekly (at weeks 2, 4, and 6 for bNAb-only animals and at weeks 9, 11, and 13 for cART-plus-bNAb animals).

Quantitation of plasma viral RNA levels
Viral RNA levels in plasma were determined by quantitative RT–PCR (ABI Prism 7900HT sequence detection system; Applied Biosystems) as previously described (Endo et al., 2000).

Lymphocyte immunophenotyping
EDTA-treated blood samples were stained for flow cytometric analysis for lymphocyte immunophenotyping as previously described (Nishimura et al., 2010).

Virus sequencing
Viral RNA extraction from plasma and RT was conducted as described with modifications (Imamichi et al., 2002). Briefly, viral RNA was isolated from macaque plasma using the QIAmp Viral RNA Isolation kit (Qiagen) and converted to cDNA using the Superscript III or Superscript IV First Strand cDNA synthesis kit (Thermo Fisher). cDNA was subject to PCR amplification for the gp120 region using Platinum PCR Supermix HiFi (Thermo Fisher) 5′-TCCTCTCTCAGCTATACCGC-3′ (nt 6129 forward) and 5′-GTGAGCTCAAGCCCTTGTC-3′ (nt 9216 reverse) primers, followed by a nested PCR reaction using 5′-AAGAGCAGAAGA CAGTGGCA-3′ (nt 6475 forward) and 5′-ATCCACCCACTAATC GCACG-3′ (nt 8730 reverse) primers (Integrated DNA Technologies). Initial denaturation was performed at 94°C for 2 min, followed by 32 cycles of 20 s at 94°C, 30 s at 55°C, and 2 min 20 s (nested) or 3 min 20 s (primary) at 68°C, with a final extension for 7 min at 68°C. PCR products were ligated into PCR4-TOPO-TA vectors using the TOPO-TA Cloning Kit (Thermo Fisher), and each ligation reaction was transformed into TOP10 Chemically competent *Escherichia coli* (Thermo Fisher) according to manufacturer's instructions. Plasmid DNA was extracted and purified using the QIAPrep SpinPrep miniprep kit (Qiagen). Sequences were aligned using MacVector sequence analysis software (MacVector Inc.) starting from the first three codons of gp120 (ATGAAAGTG) and stopping after nt 8730 regardless of primers used. Sequence alignments were evaluated using the Model Tool in MEGA X for macOS (Stecher et al., 2020) to find the most appropriate substitution modeling parameters, for which the software recommended the Hasegawa-Kishino-Yano model with Gamma distribution and invariant rate among sites (HKY+G+I; Hasegawa et al., 1985). These recommended parameters were used to reconstruct a maximum likelihood tree in MEGA X inferred via extensive subtree pruning and regrafting (SPR level 5) and 1,000 bootstrap replicates for branch support. The resulting tree was colorized using the Rainbow Tree tool (Los Alamos National Laboratory), and bootstrap values >70% are indicated at the start of each clade. The viral sequences recovered from infected macaques have been deposited in GenBank under accession numbers MT864360–MT864599.

LN processing
LN biopsies were placed in RPMI-1640 medium. After removal of fat and connective, the tissue was cut into small pieces and dissociated with the plastic end of a 6-ml syringe plunger. Cell suspensions were passed through a 40-μm cell strainer and washed twice in RPMI-1640 medium supplemented with 10% FBS, 100 U/ml penicillin, 100 μg/ml streptomycin, and 2 mM L-glutamine (complete medium). Cells were frozen in FBS containing 10% DMSO and stored in liquid nitrogen until further use.

Functional assays of CD8+ T cells in LN
Thawed LN cells were suspended in complete medium for 1 h at 37°C/5% CO$_2$. The cells were then stimulated for 6 h at 37°C/5% CO$_2$ with 4 μg/ml SIV Gag peptide pool in the presence of monensin (GolgiStop; BD Biosciences), brefeldin A (Sigma), and anti-CD107a antibody (clone H4A3; Biolegend) for the

Nishimura et al.
NAb treatment generates durable cellular immunity

Journal of Experimental Medicine   6 of 8
https://doi.org/10.1084/jem.20201214

assessment of cellular degranulation. The unstimulated condition (with DMSO instead of SIV Gag peptide pool) was included for all samples. For each functional readout, the frequency of SIV Gag–specific stimulated cells was background (unstimulated condition) subtracted.

Flow cytometry for intracellular cytokine staining

Cells were surface stained with Aqua amine viability dye (Invitrogen) for 10 min at room temperature, followed by surface staining with directly conjugated and biotinylated antibodies for 15 min at room temperature and streptavidin-BV421 (Biolegend) incubation for 15 min at room temperature. Washes between and following the surface staining steps were performed in FACS buffer (PBS containing 2% FBS). Cells were fixed and permeabilized in Cytofix/Cytoperm (BD Biosciences) for 30 min at 4°C, washed in Perm/Wash buffer (BD Biosciences), and stained intracellularly with directly conjugated antibodies for 30 min at 4°C.

The cells were washed in Perm/Wash buffer and resuspended in FACS buffer before data acquisition. Samples were acquired on a modified BD FACSymphony (BD Biosciences) equipped with 355-, 405-, 488-, 532-, and 628-nm lasers. Data were analyzed using FlowJo software version 9.9.6 (BD Biosciences). The antibodies used for intracellular cytokine staining are shown in Fig. S5. The gating strategy for functional readouts was evaluated in either total CD8+ or fCD8+ T cells (identified as live CD3+CD8+CCR7−CD95hiCXCR5+ cells) as shown in Fig. S5. Within each of these cell populations, the functional readouts were evaluated as either coexpression of CD69 and cytokine (IFN-γ, TNF, or MIP-1β) or total CD107a expression. The polyfunctionality analyses were performed using the Simple Presentation of Incredibly Complex Evaluations software v.6.0 (Vaccine Research Center, National Institute of Allergy and Infectious Diseases, National Institutes of Health).

Online supplemental material

Fig. S1 shows CD4+ T cell levels in macaques treated with bNAbs alone or cART plus bNAbs. Fig. S2 describes *env* gene diversity in SHIV-infected macaques following initiation of bNAb immunotherapy on day 3 PI. Fig. S3 demonstrates that follicular CXCR5+ CD8+ T cell accumulation and SIV-specific CD8+ T cell responses in LNs from the controller macaques occurred following combination bNAb therapy beginning on day 3 PI, but not in the controller macaques following bNAb ± cART treatment beginning at week 2 PI. Fig. S4 displays polyfunctional profiles of bulk CD8+ and follicular CXCR5+ CD8+ T cell responses to SIV Gag in the LNs of day 3 controller, progressor, and cART-only treated monkeys. Fig. S5 lists the antibodies used for intracellular cytokine staining and the gating strategy used to define CCR7loCD95hiCXCR5hi fCD8+ cells in flow cytometry datasets.

Acknowledgments

Disclosures: The authors declare no competing interests exist.

References

Betts, M.R., M.C. Nason, S.M. West, S.C. De Rosa, S.A. Migueles, J. Abraham, M.M. Lederman, J.M. Benito, P.A. Goepfert, M. Connors, et al. 2006. HIV nonprogressors preferentially maintain highly functional HIV-specific CD8+ T cells. *Blood.* 107:4781–4789. https://doi.org/10.1182/blood-2005-12-4818

Borducchi, E.N., J. Liu, J.P. Nkolola, A.M. Cadena, W.H. Yu, S. Fischinger, T. Broge, P. Abbink, N.B. Mercado, A. Chandrashekar, et al. 2018. Antibody and TLR7 agonist delay viral rebound in SHIV-infected monkeys. *Nature.* 563:360–364. https://doi.org/10.1038/s41586-018-0600-6

Caskey, M., F. Klein, J.C. Lorenzi, M.S. Seaman, A.P. West, Jr., N. Buckley, G. Kremer, L. Nogueira, M. Braunschweig, J.F. Scheid, et al. 2015. Viraemia suppressed in HIV-1-infected humans by broadly neutralizing antibody 3BNC117. *Nature.* 522:487–491. https://doi.org/10.1038/nature14411

Caskey, M., T. Schoofs, H. Gruell, A. Settler, T. Karagounis, E.F. Kreider, B. Murrell, N. Pfeifer, L. Nogueira, T.Y. Oliveira, et al. 2017. Antibody 10-1074 suppresses viremia in HIV-1-infected individuals. *Nat. Med.* 23:185–191. https://doi.org/10.1038/nm.4268

Deeks, S.G., and B.D. Walker. 2007. Human immunodeficiency virus controllers: mechanisms of durable virus control in the absence of antiretroviral therapy. *Immunity.* 27:406–416. https://doi.org/10.1016/j.immuni.2007.08.010

Endo, Y., T. Igarashi, Y. Nishimura, C. Buckler, A. Buckler-White, R. Plishka, D.S. Dimitrov, and M.A. Martin. 2000. Short- and long-term clinical outcomes in rhesus monkeys inoculated with a highly pathogenic chimeric simian/human immunodeficiency virus. *J. Virol.* 74:6935–6945. https://doi.org/10.1128/JVI.74.15.6935-6945.2000

Ferrando-Martinez, S., E. Moysi, A. Pegu, S. Andrews, K. Nganou Makamdop, D. Ambrozak, A.B. McDermott, D. Palesch, M. Paiardini, G.N. Pavlakis, et al. 2018. Accumulation of follicular CD8+ T cells in pathogenic SIV infection. *J. Clin. Invest.* 128:2089–2103. https://doi.org/10.1172/JCI96207

Gautam, R., Y. Nishimura, A. Pegu, M.C. Nason, F. Klein, A. Gazumyan, J. Golijanin, A. Buckler-White, R. Sadjadpour, K. Wang, et al. 2016. A single injection of anti-HIV-1 antibodies protects against repeated SHIV challenges. *Nature.* 533:105–109. https://doi.org/10.1038/nature17677

Gautam, R., Y. Nishimura, N. Gaughan, A. Gazumyan, T. Schoofs, A. Buckler-White, M.S. Seaman, B.J. Swihart, D.A. Follmann, M.C. Nussenzweig, et al. 2018. A single injection of crystallizable fragment domain-modified

antibodies elicits durable protection from SHIV infection. *Nat. Med.* 24: 610–616. https://doi.org/10.1038/s41591-018-0001-2

Hasegawa, M., H. Kishino, and T. Yano. 1985. Dating of the human-ape splitting by a molecular clock of mitochondrial DNA. *J. Mol. Evol.* 22: 160–174. https://doi.org/10.1007/BF02101694

Hessell, A.J., J.P. Jaworski, E. Epson, K. Matsuda, S. Pandey, C. Kahl, J. Reed, W.F. Sutton, K.B. Hammond, T.A. Cheever, et al. 2016. Early short-term treatment with neutralizing human monoclonal antibodies halts SHIV infection in infant macaques. *Nat. Med.* 22:362–368. https://doi.org/10.1038/nm.4063

Imamichi, H., T. Igarashi, T. Imamichi, O.K. Donau, Y. Endo, Y. Nishimura, R.L. Willey, A.F. Suffredini, H.C. Lane, and M.A. Martin. 2002. Amino acid deletions are introduced into the V2 region of gp120 during independent pathogenic simian immunodeficiency virus/HIV chimeric virus (SHIV) infections of rhesus monkeys generating variants that are macrophage tropic. *Proc. Natl. Acad. Sci. USA.* 99:13813–13818. https://doi.org/10.1073/pnas.212511599

Ledgerwood, J.E., E.E. Coates, G. Yamshchikov, J.G. Saunders, L. Holman, M.E. Enama, A. DeZure, R.M. Lynch, I. Gordon, S. Plummer, et al; VRC 602 Study Team. 2015. Safety, pharmacokinetics and neutralization of the broadly neutralizing HIV-1 human monoclonal antibody VRC01 in healthy adults. *Clin. Exp. Immunol.* 182:289–301. https://doi.org/10.1111/cei.12692

Lu, C.L., D.K. Murakowski, S. Bournazos, T. Schoofs, D. Sarkar, A. Halper-Stromberg, J.A. Horwitz, L. Nogueira, J. Golijanin, A. Gazumyan, et al. 2016. Enhanced clearance of HIV-1-infected cells by broadly neutralizing antibodies against HIV-1 in vivo. *Science.* 352:1001–1004. https://doi.org/10.1126/science.aaf1279

Lynch, R.M., E. Boritz, E.E. Coates, A. DeZure, P. Madden, P. Costner, M.E. Enama, S. Plummer, L. Holman, C.S. Hendel, et al; VRC 601 Study Team. 2015. Virologic effects of broadly neutralizing antibody VRC01 administration during chronic HIV-1 infection. *Sci. Transl. Med.* 7. 319ra206. https://doi.org/10.1126/scitranslmed.aad5752

Moldt, B., E.G. Rakasz, N. Schultz, P.Y. Chan-Hui, K. Swiderek, K.L. Weisgrau, S.M. Piaskowski, Z. Bergman, D.I. Watkins, P. Poignard, et al. 2012. Highly potent HIV-specific antibody neutralization in vitro translates into effective protection against mucosal SHIV challenge in vivo. *Proc. Natl. Acad. Sci. USA.* 109:18921–18925. https://doi.org/10.1073/pnas.1214785109

Mouquet, H., L. Scharf, Z. Euler, Y. Liu, C. Eden, J.F. Scheid, A. Halper-Stromberg, P.N. Gnanapragasam, D.I. Spencer, M.S. Seaman, et al. 2012. Complex-type N-glycan recognition by potent broadly neutralizing HIV antibodies. *Proc. Natl. Acad. Sci. USA.* 109:E3268–E3277. https://doi.org/10.1073/pnas.1217207109

Niessl, J., A.E. Baxter, P. Mendoza, M. Jankovic, Y.Z. Cohen, A.L. Butler, C.L. Lu, M. Dubé, I. Shimeliovich, H. Gruell, et al. 2020. Combination anti-HIV-1 antibody therapy is associated with increased virus-specific T cell immunity. *Nat. Med.* 26:222–227. https://doi.org/10.1038/s41591-019-0747-1

Nishimura, Y., M. Shingai, R. Willey, R. Sadjadpour, W.R. Lee, C.R. Brown, J.M. Brenchley, A. Buckler-White, R. Petros, M. Eckhaus, et al. 2010. Generation of the pathogenic R5-tropic simian/human immunodeficiency virus SHIVAD8 by serial passaging in rhesus macaques. *J. Virol.* 84:4769–4781. https://doi.org/10.1128/JVI.02279-09

Nishimura, Y., R. Gautam, T.W. Chun, R. Sadjadpour, K.E. Foulds, M. Shingai, F. Klein, A. Gazumyan, J. Golijanin, M. Donaldson, et al. 2017. Early antibody therapy can induce long-lasting immunity to SHIV. *Nature.* 543:559–563. https://doi.org/10.1038/nature21435

Pereyra, F., M.M. Addo, D.E. Kaufmann, Y. Liu, T. Miura, A. Rathod, B. Baker, A. Trocha, R. Rosenberg, E. Mackey, et al. 2008. Genetic and immunologic heterogeneity among persons who control HIV infection in the absence of therapy. *J. Infect. Dis.* 197:563–571. https://doi.org/10.1086/526786

Petrovas, C., S. Ferrando-Martinez, M.Y. Gerner, J.P. Casazza, A. Pegu, C. Deleage, A. Cooper, J. Hataye, S. Andrews, D. Ambrozak, et al. 2017. Follicular CD8 T cells accumulate in HIV infection and can kill infected cells in vitro via bispecific antibodies. *Sci. Transl. Med.* 9. eaag2285. https://doi.org/10.1126/scitranslmed.aag2285

Scheid, J.F., H. Mouquet, B. Ueberheide, R. Diskin, F. Klein, T.Y. Oliveira, J. Pietzsch, D. Fenyo, A. Abadir, K. Velinzon, et al. 2011. Sequence and structural convergence of broad and potent HIV antibodies that mimic CD4 binding. *Science.* 333:1633–1637. https://doi.org/10.1126/science.1207227

Shingai, M., O.K. Donau, S.D. Schmidt, R. Gautam, R.J. Plishka, A. Buckler-White, R. Sadjadpour, W.R. Lee, C.C. LaBranche, D.C. Montefiori, et al. 2012. Most rhesus macaques infected with the CCR5-tropic SHIV(AD8) generate cross-reactive antibodies that neutralize multiple HIV-1 strains. *Proc. Natl. Acad. Sci. USA.* 109:19769–19774. https://doi.org/10.1073/pnas.1217443109

Shingai, M., Y. Nishimura, F. Klein, H. Mouquet, O.K. Donau, R. Plishka, A. Buckler-White, M. Seaman, M. Piatak, Jr., J.D. Lifson, et al. 2013. Antibody-mediated immunotherapy of macaques chronically infected with SHIV suppresses viraemia. *Nature.* 503:277–280. https://doi.org/10.1038/nature12746

Shingai, M., O.K. Donau, R.J. Plishka, A. Buckler-White, J.R. Mascola, G.J. Nabel, M.C. Nason, D. Montefiori, B. Moldt, P. Poignard, et al. 2014. Passive transfer of modest titers of potent and broadly neutralizing anti-HIV monoclonal antibodies block SHIV infection in macaques. *J. Exp. Med.* 211:2061–2074. https://doi.org/10.1084/jem.20132494

Stecher, G., K. Tamura, and S. Kumar. 2020. Molecular Evolutionary Genetics Analysis (MEGA) for macOS. *Mol. Biol. Evol.* 37:1237–1239. https://doi.org/10.1093/molbev/msz312
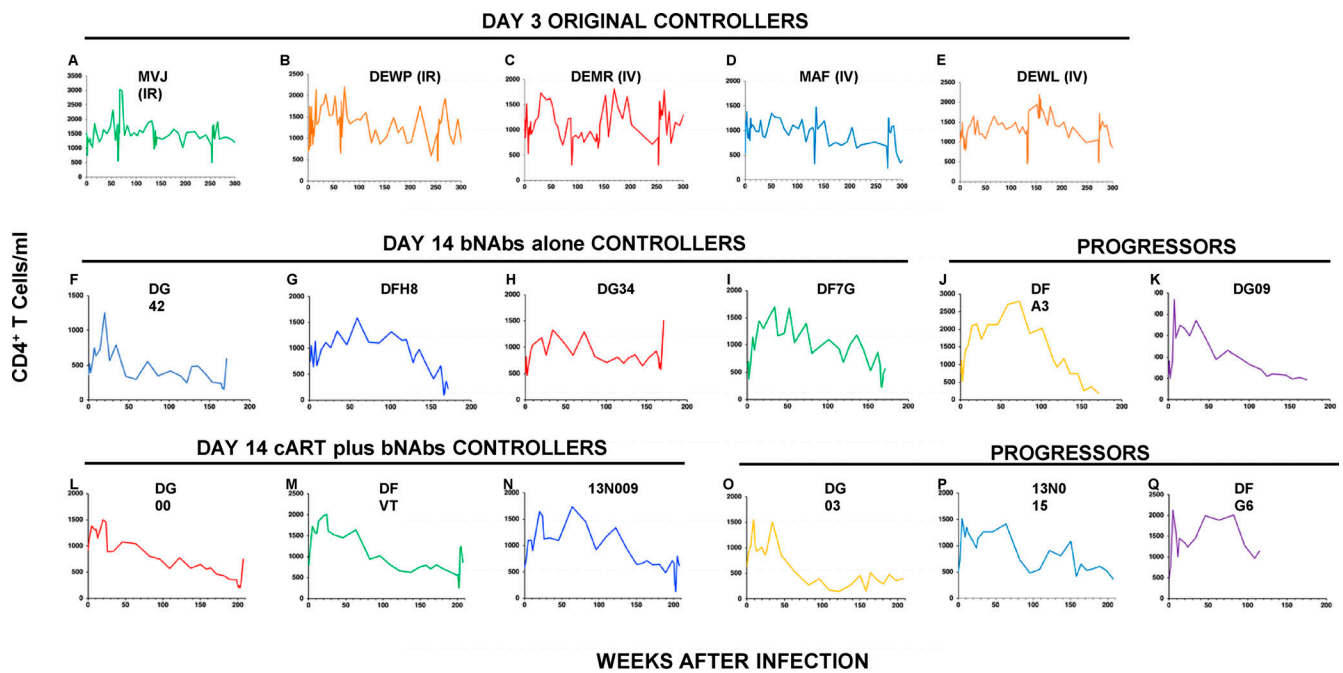
Figure S1. **CD4+ T cell levels in macaques treated with bNAbs alone or cART plus bNAbs. (A–Q)** Absolute numbers of circulating CD4+ T cells in five controller macaques following bNAb therapy beginning on day 3 PI (A–E); in four controller (F–I) and two progressor (J and K) macaques following bNAb therapy alone beginning at week 2 PI; and in three controller (L–N) and three progressor (O–Q) macaques after cART plus bNAb therapy beginning at week 2 PI are shown.
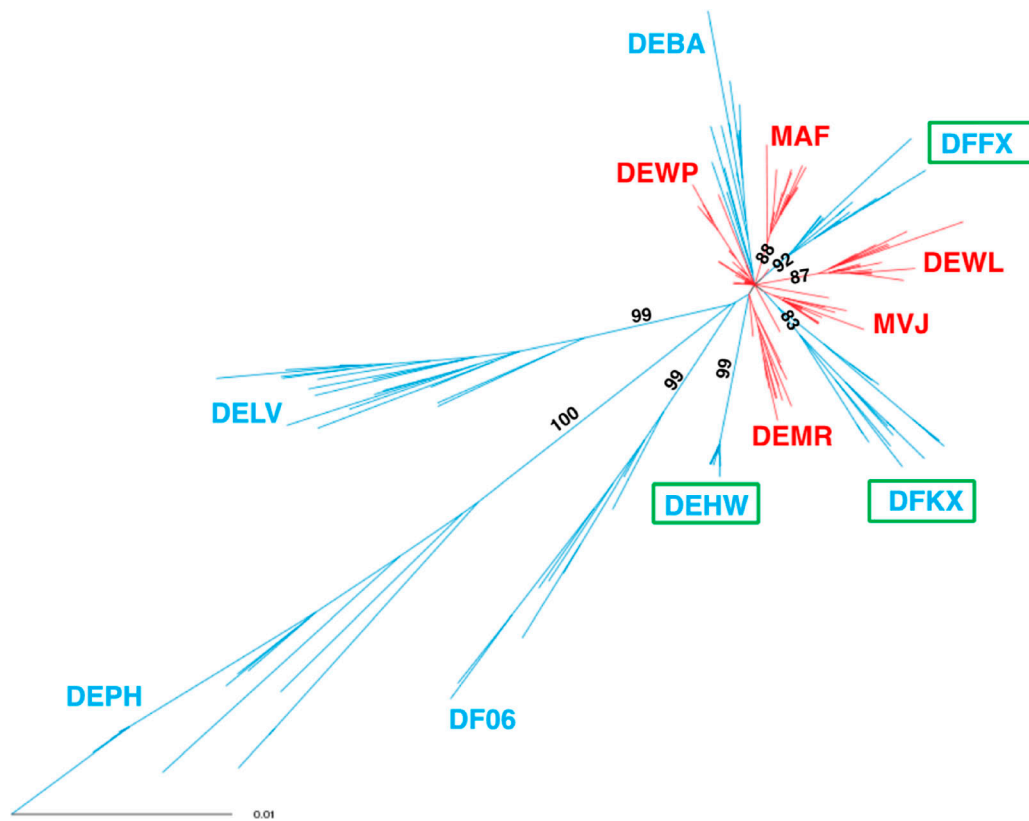
Figure S2.   ***Env* gene diversity in SHIV-infected macaques following initiation of bNAb immunotherapy on day 3 PI.** An unrooted phylogram of *env* gene sequences displays phylogenetic diversity in controllers (red) at weeks 70–130 PI, in late controllers (green rectangles) at weeks 110–150 PI, and in progressors (blue) at weeks 110–150 PI. Diversity of 0.01 is indicated. Branch lengths were measured by the number of substitutions per site. Bootstrap numbers >70% are indicated at the start of each clade.
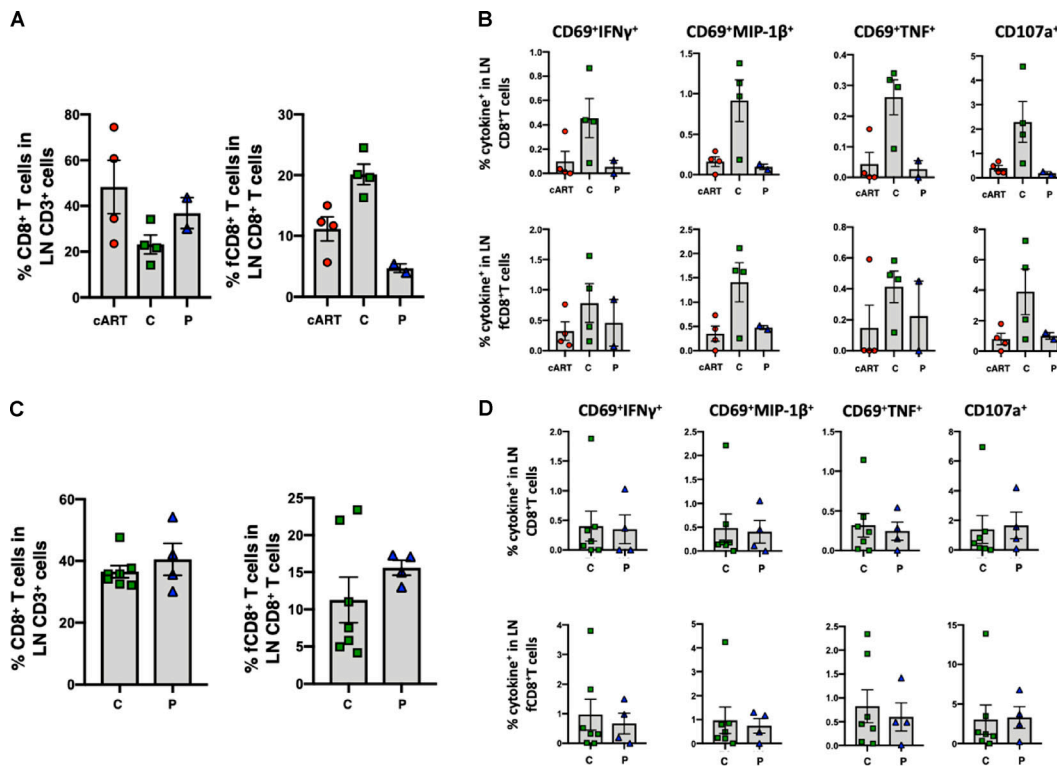
Figure S3. Follicular CXCR5+ CD8+ T cell accumulation and SIV-specific CD8+ T cell responses in LNs from the controller macaques occur following combination bNAb therapy beginning on day 3 PI, but not in the controller macaques following bNAb ± cART treatment beginning at week 2 PI. (A–D) Treatments were initiated on day 3 (A and B) or at week 2 (C and D). **(A)** Follicular CXCR5+ CD8+ T cells accumulated in LNs of day 3 controller (C) animals (*n* = 4) compared with the same T cell subset collected from progressor (P) macaques (*n* = 2) or control monkeys treated with cART only, starting at day 3 (*n* = 4). Comparable fractions of bulk CD8+ T cells were present in LNs from the three groups of monkeys. The Kruskal-Wallis test followed by Dunn's multiple comparisons test showed a statistically significant difference in levels of fCD8+ T cells between controller and progressor monkeys (P = 0.0228). **(B)** Antiviral responses in both bulk and follicular CXCR5+ CD8+ T cells in LNs from controller macaques were higher than in LNs from progressor or cART-only control macaques. The CD8+ T cell responses to SIVmac239 Gag were measured by intracellular cytokine staining (IFN-γ, MIP-1β, TNF, and CD107a). **(C)** The fractions of follicular CXCR5+ CD8+ T cells in LNs from controller (*n* = 7) and progressor (*n* = 4) animals were comparable. **(D)** Antiviral responses in both bulk and follicular CXCR5+ CD8+ T cells in LNs from controller macaques were comparable to the responses measured in progressor animals. The CD8+ T cell responses to SIVmac239 Gag were measured by intracellular cytokine staining (IFN-γ, MIP-1β, TNF, and CD107a). Error bars indicate SD of data from multiple animals.

Figure S4. **Polyfunctional profile of bulk CD8+ and follicular CXCR5+ CD8+ T cell responses to SIV Gag in the LNs of day 3 controller, progressor, and cART-only monkeys.** The pie charts and graphs show the mean frequency of cells performing all different combinations of effector functions. Graphs also show the individual data points. C, controller macaques; P, progressor macaques.

Antibodies for intracellular cytokine assays

Ab specificity	Fluorochrome	Clone	Company
CD107a	BV650	H4A3	Biolegend
CD20	BV510	2H7	Biolegend
CD16	BV510	3G8	Biolegend
CD14	BV510	M5E2	Biolegend
CD8	BV570	RPA-T8	Biolegend
CD28	ECD	CD28.2	Beckman Coulter
CD95	PE-Cy5	DX2	BD Biosciences
CXCR5	Biotin	MU5UBEE	eBioscience
CCR7	AF700	150503	BD Biosciences
PD-1	BV711	EH12.2H7	Biolegend
IFNγ	FITC	B27	BD Biosciences
TNF	BV785	Mab11	Biolegend
MIP-1β	PE	D21-1351	BD Biosciences
CD69	BV605	FN50	Biolegend
CD3	APC-Cy7	SP34-2	BD Biosciences

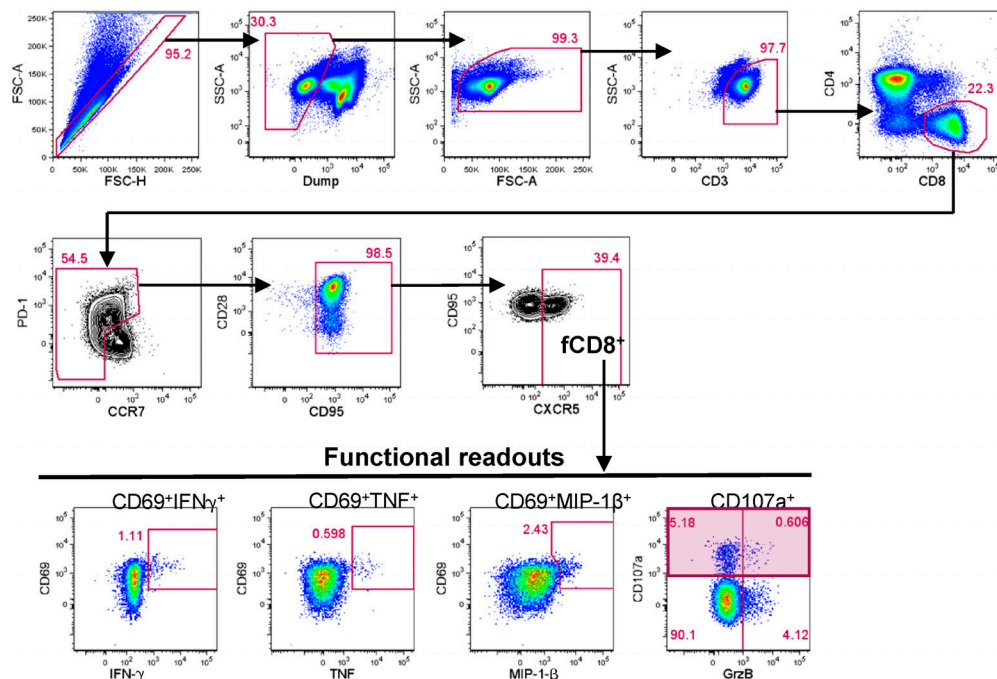## Gating strategy (representative example)

Functional readouts

Figure S5. **Antibodies used for intracellular cytokine staining and gating strategy used to define CCR7^{lo}CD95^{hi}CXCR5^{hi} fCD8$^+$ cells in flow cytometry datasets.** Representative flow cytometry plots from one representative animal are shown. Functional readouts were evaluated as either coexpression of CD69 and cytokine (IFN-γ, TNF, or MIP-1β) or total CD107a expression. Ab, antibody; ECD, electron coupled dye; FSC, forward scatter; SSC, side scatter.